

Electronic Supporting Information

Unprecedented boat-shaped $[Mo_2O_5(VO_3)_4]^{2-}$ polyanions induced strong second harmonic generation response [†]

Wei Zeng,^a Xuehua Dong,^a Yao Tian,^a Ling Huang,^b Hongmei Zeng,^a Zhien Lin,^{*a} and Guohong Zou^{*a}

^aCollege of Chemistry, Sichuan University, Chengdu 610065, P. R. China

^bCollege of Chemistry and Materials Science, Sichuan Normal University, Chengdu 610066, P. R. China

Table of contents

Sections	Titles	Pages
Sections S1	Experimental section (Instrumentations and Computational Descriptions).	S3-S5
Table S1	Crystal data and structure refinement for GMIO.	S6
Table S2	Atomic coordinates and equivalent isotropic displacement parameters for GMIO.	S7
Table S3	Selected Bond lengths (Å) and angles (deg) for GMIO.	S8
Table S4	Calculation of dipole moment for IO_3 , MoO_6 , $\text{C}(\text{NH}_2)_3$ polyhedra and net dipole moment for a unit cell in GMIO (D = Debyes).	S9-S10
Table S5	Structures, Band gaps and SHG intensities of existing NCS molybdenum (VI) iodate (V).	S11
Fig. S1	boat-shaped $[\text{Mo}_2\text{O}_5(\text{IO}_3)_4]^{2-}$ polyanion.	S12
Fig. S2	Illustration of the 3D structure of GMIO viewed down the a-axis. Green arrows indicate the direction of the dipole moments.	S12
Fig. S3	Experimental and calculated XRD patterns for GMIO.	S13
Fig. S4	TGA analysis of GMIO under N_2 atmosphere.	S13
Fig. S5	The IR spectrum of GMIO.	S13
Fig. S6	Calculated band structures for GMIO.	S14
References		S15

Section S1. Experimental Section

Synthesis.

The starting material $[\text{C}(\text{NH}_2)_3]_2\text{CO}_3$ (99%, Aladdin), HIO_3 (99.5%, MACKLIN) and MoO_3 (99.5%, MACKLIN) were commercially available with analytical grade and used without further processing.

$[\text{C}(\text{NH}_2)_3]_2\text{CO}_3$ (0.090 g, 0.5 mmol), HIO_3 (0.352 g, 2 mmol) and MoO_3 (0.072 g, 0.5 mmol) were sealed in a 23 mL Teflon-lined steel autoclave with H_2O (2 mL) and then heated at 85 °C for 4 days. The autoclave was cooled to room temperature with the rate of 6 °C/h, colorless plate crystals of $[\text{C}(\text{NH}_2)_3]_2\text{Mo}_2\text{O}_5(\text{IO}_3)_4 \cdot 2\text{H}_2\text{O}$ (GMIO) were obtained in ~78% yield (based on Mo).

Instrumentations.

Single crystal X-ray diffraction.

The diffraction data of GMIO was measured on a Rigaku XtaLAB Synergy R diffractometer with Mo K α ($\lambda = 0.71073\text{\AA}$) radiation at 293(2) K. The structure was solved and refined on F^2 using the SHELX-2015 program package.^{1,2} All of the structures were verified using the PLATON and no higher symmetries were found.³ Crystallographic data and structural refinements for GMIO are summarized in Table S1. Crystallographic data details are listed in Tables S2-S3 in the ESI†, respectively.

Powder XRD diffraction.

In order to confirm the phase purity of GMIO, powder XRD patterns was obtained using a Rigaku Smartlab powder X-ray diffractometer with Cu K α radiation ($\lambda = 1.54056\text{\AA}$), in the angular range of $2\theta = 5\text{--}50^\circ$ (step width: 0.02°).

Thermal analysis.

Netzsch STA 409 PC thermal analyzer, with a heating rate of 10 °C /min and in the range of RT-800 °C under N_2 atmosphere was used to measure the thermal behavior of GMIO.

IR Spectroscopy.

IR spectrum of GMIO was obtained on a Vertex 70 Fourier transform infrared (FT-IR) spectrometer by using KBr pellets, with transmission mode from 4000 to 400 cm^{-1} . The power samples containing 100 mg of dry KBr and 1 mg of cleaned crystals were compressed into tablets

and measured.

UV-vis-NIR Diffuse Reflectance Spectroscopy.

UV-vis-NIR diffuse reflectance spectrum of GMIO was recorded by using PerkinElmer Lambda-950 UV/VIS/NIR spectrophotometer at room temperature. The Kubelka-Munk function^{4,5} is used to calculate the absorption spectrum from the reflection spectrum: $F(R) = \alpha/S = (1-R)^2/2R$, where R is the reflectance, α is the absorption coefficient, and S is the scattering coefficient.

Second-Harmonic Generation Tests.

A Q-switched Nd: YAG laser was used to measure the SHG signals of GMIO and KDP under 1064 nm radiation based on Kurtz-Perry method.⁶ Crystalline GMIO and KDP were ground and sieved into the following particle size: 25-45, 45-58, 58-75, 75-106, 106-150, and 150-212 μm owing to that the SHG efficiency mainly depends on the particle size.

Computational Descriptions.

The first-principles calculations were carried out on GMIO by using the CASTEP.⁷ The gradient-corrected functional (GGA) with Perdew-Burke-Ernzer (PBE) was used for all the calculations.⁸ All the atoms were performed by Norm-conserving pseudopotentials (NCP), with C 2s²2p², N 2s²2p³ Mo 4d⁵s¹, I 4d¹⁰5s²5p⁵, O 2s²2p⁴ treated as valence electrons.⁹ The kinetic energy cutoff of 750 eV and the k-point sampling of $1 \times 2 \times 3$ were chosen for the GMIO.¹⁰ All other parameter settings are CASTEP default values.

To obtain the linear optical properties, the complex dielectric function $\varepsilon(\omega) = \varepsilon_1(\omega) + i\varepsilon_2(\omega)$ has been determined in the random phase approximation from the PBE wavefunctions. The imaginary part of the dielectric function due to direct inter-band transitions is given by the expression,

$$\varepsilon_2(\hbar\omega) = \frac{2e^2\pi}{\Omega\varepsilon_0} \sum_{k,v,c} \left| \langle \psi_k^c | u \cdot r | \psi_k^v \rangle \right|^2 \delta(E_k^c - E_k^v - E)$$

where Ω , ω , u , v and c are the unit-cell volume, photon frequencies, the vector defining the polarization of the incident electric field, valence and conduction bands, respectively. The real part of the dielectric function is obtained from ε_2 by a Kramers-Kronig transformation,

$$\varepsilon_1(\omega) = 1 + \left(\frac{2}{\pi} \right) \int_0^{+\infty} d\omega' \frac{\omega'^2 \varepsilon_2(\omega)}{\omega'^2 - \omega^2}$$

In calculation of the static $\chi^{(2)}$ coefficients, the so-called length-gauge formalism derived by

Aversa and Sipe¹¹ and modified by Rashkeev *et al*¹² is adopted, which has been proved to be successful in calculating the second order susceptibility for semiconductors and insulators.^{13, 14} In the static case, the imaginary part of the static second-order optical susceptibility can be expressed as:

$$\begin{aligned} \chi^{abc} &= \frac{e^3}{\hbar^2 \Omega} \sum_{nml,k} \frac{r_{nm}^a (r_{ml}^b r_{ln}^c + r_{ml}^c r_{ln}^b)}{2\omega_{nm} \omega_{ml} \omega_{ln}} [\omega_n f_{ml} + \omega_m f_{ln} + \omega_l f_{nm}] \\ &\quad + \frac{ie^3}{4\hbar^2 \Omega} \sum_{nm,k} \frac{f_{nm}}{\omega_{nm}^2} [r_{nm}^a (r_{mn;c}^b + r_{mn;b}^c) + r_{nm}^b (r_{mn;c}^a + r_{mn;a}^c) + r_{nm}^c (r_{mn;b}^a + r_{mn;a}^b)] \end{aligned}$$

where r is the position operator, $\hbar\omega_{nm} = \hbar\omega_n - \hbar\omega_m$ is the energy difference for the bands m and n , $f_{mn} = f_m - f_n$ is the difference of the Fermi distribution functions, subscripts a, b , and c are Cartesian indices, and $r_{mn;a}^b$ is the so-called generalized derivative of the coordinate operator in k space,

$$r_{nm;a}^b = \frac{r_{nm}^a \Delta_{mn}^b + r_{nm}^b \Delta_{mn}^a}{\omega_{nm}} + \frac{i}{\omega_{nm}} \times \sum_l (\omega_{lm} r_{nl}^a r_{lm}^b - \omega_{nl} r_{nl}^b r_{lm}^a)$$

where $\Delta_{nm}^a = (p_{nm}^a - p_{mm}^a) / m$ is the difference between the electronic velocities at the bands n and m .

Table S1. Crystal data and structure refinement for GMIO.

Compound	[C(NH₂)₃]₂Mo₂O₅(IO₃)₄·2H₂O
Formula Mass	1126.68
Crystal System	orthorhombic
Space Group	<i>Pna</i> 2 ₁
a (Å)	23.8979 (5)
b (Å)	13.1994 (3)
c (Å)	7.8514 (2)
α (°)	90
β (°)	90
γ (°)	90
V(Å³)	2476.63 (10)
Z	4
ρ(calcd) (g/cm³)	3.022
Temperature (K)	293 (2)
λ (Å)	0.71073
F(000)	2068.0
μ (mm⁻¹)	6.087
Final <i>R</i> indices (<i>I</i>>2σ(<i>I</i>))^a <i>R</i>_{<i>I</i>}/w<i>R</i>₂	0.0314/0.0882
GOF on <i>F</i>²	1.083
Flack factor	0.06 (3)

^a*R*_{*I*}(*F*) = $\sum |F_o - |F_c|| / \sum |F_o|$, w*R*₂(*F*_{*o*}²) = $[\sum w(F_o^2 - F_c^2)^2 / \sum w(F_o^2)^2]^{1/2}$

Table S2. Atomic coordinates and equivalent isotropic displacement parameters for GMIO. $U_{(\text{eq})}$ is defined as one third of the trace of the orthogonalized U_{ij} tensor.

atom	x	y	z	$U_{\text{eq}} (\text{\AA}^2)$
I1	0.71556 (2)	0.49881 (4)	0.48843 (7)	0.02004 (13)
I2	0.71402 (2)	0.76550 (4)	0.72593 (7)	0.01682 (13)
I3	0.69495 (2)	0.76610 (4)	0.23365 (8)	0.01833 (13)
I4	0.71854 (2)	1.03055 (4)	0.47929 (8)	0.02188 (14)
Mo1	0.59125 (3)	0.62824 (6)	0.52477 (12)	0.02436 (19)
Mo2	0.59286 (3)	0.90888 (6)	0.52292 (12)	0.02286 (18)
N1	0.6447 (10)	0.2397 (16)	0.822 (5)	0.184 (17)
N1	0.6447 (10)	0.2397 (16)	0.822 (5)	0.184 (17)
N2	0.5562 (6)	0.1940 (12)	0.754 (3)	0.097 (7)
N3	0.5748 (6)	0.3584 (9)	0.808 (2)	0.087 (6)
N4	0.6294 (7)	0.2588 (11)	0.247 (4)	0.116 (10)
N5	0.5401 (6)	0.1971 (14)	0.257 (3)	0.130 (11)
N6	0.5563 (5)	0.3607 (10)	0.339 (2)	0.085 (5)
O1	0.7290 (4)	0.4079 (7)	0.6498 (11)	0.041 (2)
O2	0.7164 (3)	0.4200 (6)	0.3008 (10)	0.0341 (18)
O3	0.6384 (3)	0.4971 (4)	0.5115 (10)	0.0245 (14)
O4	0.5571 (3)	0.5919 (6)	0.7029 (12)	0.044 (2)
O5	0.5467 (3)	0.5928 (6)	0.3695 (13)	0.044 (2)
O6	0.6654 (3)	0.6623 (5)	0.6871 (8)	0.0235 (14)
O7	0.7510 (3)	0.7652 (5)	0.5257 (10)	0.0264 (14)
O8	0.6672 (3)	0.8737 (5)	0.6850 (8)	0.0227 (14)
O9	0.6559 (3)	0.6601 (5)	0.3224 (9)	0.0246 (14)
O10	0.6622 (4)	0.7660 (5)	0.0285 (10)	0.0307 (16)
O11	0.6568 (3)	0.8722 (5)	0.3237 (9)	0.0247 (15)
O12	0.5784 (3)	0.7680 (5)	0.5252 (12)	0.0305 (17)
O13	0.5476 (4)	0.9466 (7)	0.3707 (11)	0.043 (2)
O14	0.5603 (3)	0.9483 (6)	0.7045 (11)	0.0384 (18)
O15	0.6417 (3)	1.0371 (5)	0.5087 (9)	0.0267 (15)
O16	0.7349 (4)	1.1232 (6)	0.6358 (12)	0.043 (2)
O17	0.7212 (4)	1.1059 (6)	0.2880 (10)	0.0372 (19)
O18	0.6620 (4)	0.5176 (7)	0.9707 (13)	0.053 (2)
O19	0.8276 (4)	0.5121 (7)	0.4501 (14)	0.058 (3)
C1	0.5914 (6)	0.2648 (12)	0.788 (3)	0.060 (5)
C2	0.5754 (7)	0.2733 (14)	0.290 (4)	0.087 (8)

Table S3. Selected Bond lengths (Å) and angles (deg) for GMIO.

I2—O6	1.816 (7)	Mo1—O12	1.870 (6)
I2—O8	1.843 (7)	Mo1—O4	1.688 (8)
I2—O7	1.803 (7)	Mo1—O5	1.685 (8)
I3—O11	1.814 (7)	Mo2—O8	2.233 (7)
I3—O9	1.820 (7)	Mo2—O11	2.240 (7)
I3—O10	1.791 (8)	Mo2—O15	2.058 (6)
I1—O3	1.854 (6)	Mo2—O12	1.892 (6)
I1—O2	1.803 (7)	Mo2—O14	1.706 (8)
I1—O1	1.775 (8)	Mo2—O13	1.686 (7)
I4—O15	1.854 (7)	N3—C1	1.307 (18)
I4—O17	1.803 (8)	N4—C2	1.35 (3)
I4—O16	1.777 (8)	N2—C1	1.29 (2)
Mo1—O6	2.229 (7)	N6—C2	1.30 (2)
Mo1—O3	2.067 (6)	C2—N5	1.34 (2)
Mo1—O9	2.256 (7)	N1—C1	1.34 (3)
O6—I2—O8	99.4 (3)	O15—Mo2—O8	75.6 (3)
O7—I2—O6	99.5 (3)	O15—Mo2—O11	75.7 (2)
O7—I2—O8	98.4 (3)	O12—Mo2—O8	86.3 (3)
O11—I3—O9	100.8 (3)	O12—Mo2—O11	85.3 (3)
O10—I3—O11	97.6 (3)	O12—Mo2—O15	155.9 (3)
O10—I3—O9	96.9 (3)	O14—Mo2—O8	87.2 (3)
O2—I1—O3	94.8 (3)	O14—Mo2—O11	164.0 (3)
O1—I1—O3	95.9 (4)	O14—Mo2—O15	93.0 (3)
O1—I1—O2	101.0 (4)	O14—Mo2—O12	102.0 (4)
O17—I4—O15	96.5 (4)	O13—Mo2—O8	167.1 (4)
O16—I4—O15	95.7 (4)	O13—Mo2—O11	90.4 (4)
O16—I4—O17	100.9 (4)	O13—Mo2—O15	94.7 (4)
O6—Mo1—O9	79.7 (2)	O13—Mo2—O12	100.3 (4)
O3—Mo1—O6	76.4 (2)	O13—Mo2—O14	102.1 (4)
O3—Mo1—O9	75.4 (3)	I2—O6—Mo1	139.1 (4)
O12—Mo1—O6	86.0 (3)	I2—O8—Mo2	138.0 (3)
O12—Mo1—O3	156.3 (3)	I1—O3—Mo1	122.5 (3)
O12—Mo1—O9	86.0 (3)	I3—O11—Mo2	141.4 (4)
O4—Mo1—O6	88.1 (4)	I4—O15—Mo2	122.0 (3)
O4—Mo1—O3	93.9 (3)	I3—O9—Mo1	139.8 (4)
O4—Mo1—O9	165.3 (3)	Mo1—O12—Mo2	160.0 (4)
O4—Mo1—O12	101.5 (4)	N6—C2—N4	122.4 (16)
O5—Mo1—O6	166.5 (4)	N6—C2—N5	120.3 (16)
O5—Mo1—O3	94.3 (3)	N5—C2—N4	116.7 (18)
O5—Mo1—O9	88.6 (4)	N3—C1—N1	119.8 (17)
O5—Mo1—O12	99.9 (4)	N2—C1—N3	120.9 (16)
O5—Mo1—O4	102.4 (5)	N2—C1—N1	118.9 (17)
O8—Mo2—O11	79.1 (2)		

Table S4. Calculation of dipole moment for IO_3 , MoO_6 , $\text{C}(\text{NH}_2)_3$ polyhedra and net dipole moment for a unit cell in GMIO (D = Debyes).

GMIO				
Polar unit (aunit cell)	Dipole moment (D)			
	x-component	y-component	z-component	total magnitude
I(1) O_3	14.51460987	25.30343221	-0.279952704	29.17217775
	14.51460987	-25.30343221	-0.279952704	29.17217775
	-14.51460987	-25.30343221	-0.279952704	29.17217775
	-14.51460987	25.30343221	-0.279952704	29.17217775
	-14.51460987	25.30343221	-0.279952704	29.17217775
	14.51460987	-25.30343221	-0.279952704	29.17217775
I(2) O_3	13.99541272	0.030110721	23.43274766	27.29406798
	13.99541272	-0.030110721	23.43274766	27.29406798
	-13.99541272	0.030110721	23.43274766	27.29406798
	-13.99541272	-0.030110721	23.43274766	27.29406798
I(3) O_3	28.34354926	-0.154182033	3.00823772	28.50315861
	28.34354926	0.154182033	3.00823772	28.50315861
	-28.34354926	-0.154182033	3.00823772	28.50315861
	-28.34354926	0.154182033	3.00823772	28.50315861
I(4) O_3	13.17605882	-25.64197061	0.039671955	28.82916503
	-13.17605882	25.64197061	0.039671955	28.82916503
	13.17605882	25.64197061	0.039671955	28.82916503
	13.17605882	-25.64197061	0.039671955	28.82916503
	Ux	Uy	Uz	Ut
	0	0	104.2429131	104.2429131
Mo(1) O_6	-3.958849121	-1.64035744	0.494113367	4.313630363
	-3.958849121	1.64035744	0.494113367	4.313630363
	3.958849121	-1.64035744	0.494113367	4.313630363
	3.958849121	1.64035744	0.494113367	4.313630363
Mo(2) O_6	-4.380353894	-1.954702221	0.23567739	4.802489442
	-4.380353894	1.954702221	0.23567739	4.802489442
	4.380353894	1.954702221	0.23567739	4.802489442
	4.380353894	-1.954702221	0.23567739	4.802489442
	Ux	Uy	Uz	Ut
	0	0	2.919163029	2.919163029
C(1) N_3	-0.032278087	0.605897254	-2.499453233	2.572045843
	-0.032278087	-0.605897254	-2.499453233	2.572045843
	0.032278087	-0.605897254	-2.499453233	2.572045843
	0.032278087	0.605897254	-2.499453233	2.572045843
C(2) N_3	0.394407188	0.311586955	3.251268346	3.289891992
	0.394407188	-0.311586955	3.251268346	3.289891992
	-0.394407188	-0.311586955	3.251268346	3.289891992
	-0.394407188	0.311586955	3.251268346	3.289891992

	Ux	Uy	Uz	Ut
	0	0	3.007260454	3.007260454
Net dipole moment	0	0	110.1693366	110.1693366
Cell Volume	2476.63 (10) Å ³			

Table S5 Structures, Band gaps and SHG intensities of existing NCS molybdenum (VI) iodate (V).

Compounds	Anionic structure	Band gaps	density of IO _x groups	SHG intensities	Ref
GMIO	0D anions	[Mo₂O₅(IO₃)₄]²⁻	3.55 eV	6.2 × 10⁻³	5 × KDP
CsMoO ₂ F ₃ (IO ₂ F ₂)	0D anions	[MoO ₂ F ₃ (IO ₂ F ₂)] ²⁻	3.43 eV	4.0 × 10 ⁻³	4.5 × KDP
RbMoO ₂ F ₃ (IO ₂ F ₂)	0D anions	[MoO ₂ F ₃ (IO ₂ F ₂)] ²⁻	3.77 eV	4.4 × 10 ⁻³	5 × KDP
Ba ₂ [MoO ₃ (OH)(IO ₃) ₂]IO ₃	0D anions	[MoO ₃ (OH)(IO ₃) ₂] ³⁻	3.78 eV	10.2 × 10 ⁻³	8 × KDP
RE(MoO ₂)(IO ₃) ₄ (OH) (RE = (Nd, Sm, Eu))	0D anions	[MoO ₂ (OH)(IO ₃) ₃] ²⁻	unknown	12.4 × 10 ⁻³	350 × α-SiO ₂
LiMoO ₃ (IO ₃)	2D [MoO ₃ (IO ₃)] ⁻ layer		2.8 eV	8.1 × 10 ⁻³	4 × KDP
NH ₄ MoO ₃ (IO ₃)	3D framework	[MoO ₃ (IO ₃)] ⁻	3.26 eV	6.8 × 10 ⁻³	4.7 × KDP
KRb[(MoO ₃) ₂ (IO ₃) ₂]	3D framework	[MoO ₃ (IO ₃)] ³⁻	3.32 eV	6.5 × 10 ⁻³	8.5 × KDP
AMoO ₃ (IO ₃) (A = Rb, Cs)	3D framework	[MoO ₃ (IO ₃)] ⁻	3.1 eV	6.6 × 10 ⁻³	400 × α-SiO ₂

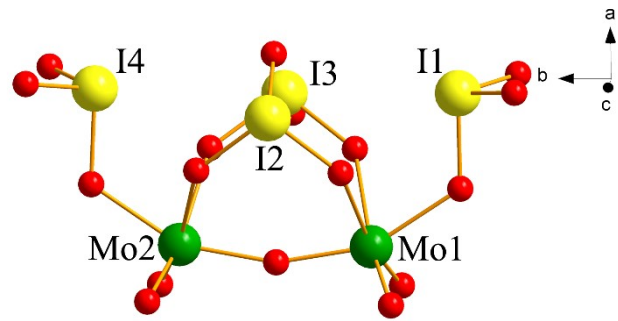


Fig. S1 boat-shaped $[\text{Mo}_2\text{O}_5(\text{VO}_4)_4]^{2-}$ polyanion.

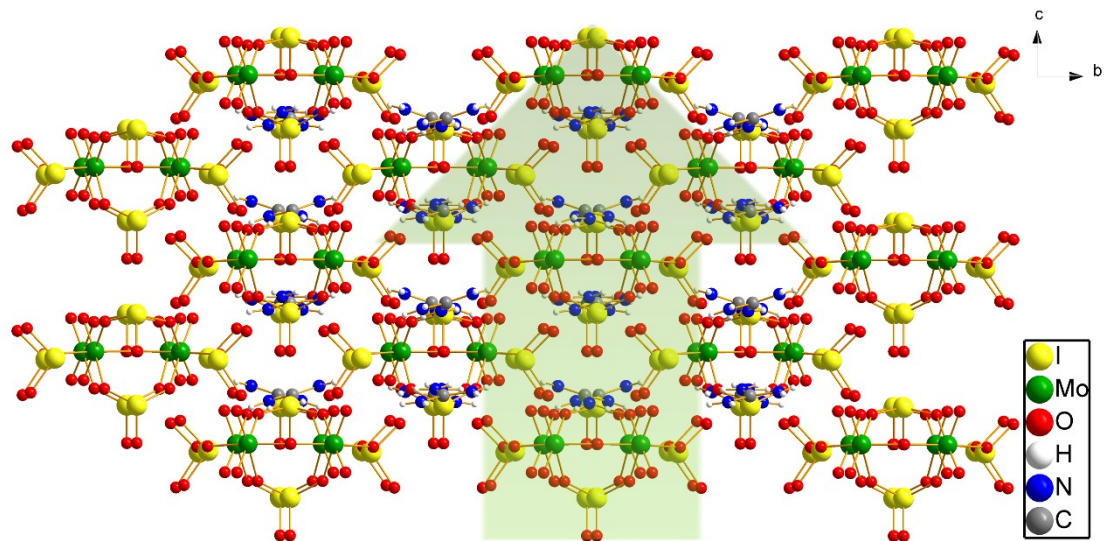


Fig. S2 Illustration of the 3D structure of GMIO viewed down the a-axis. Green arrows indicate the direction of the dipole moments.

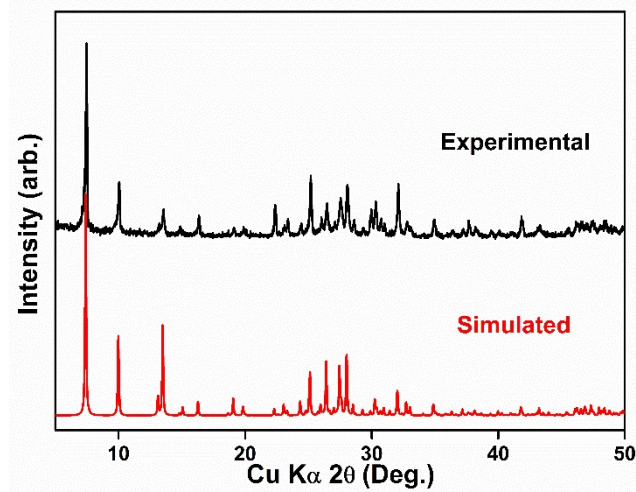


Fig. S3 Experimental and calculated XRD patterns for GMIO.

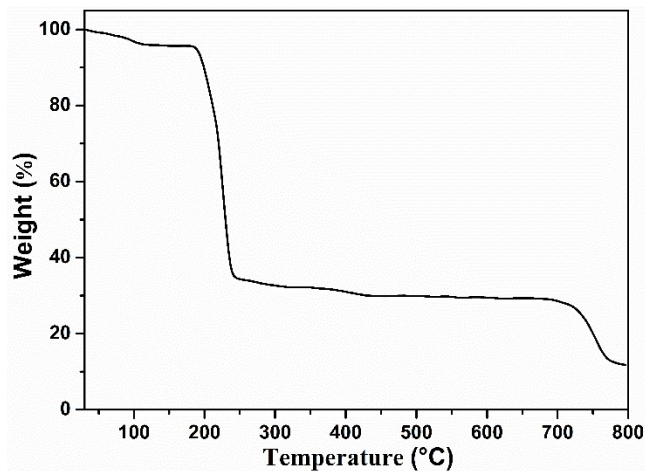


Fig. S4 TGA analysis of GMIO under N₂ atmosphere.

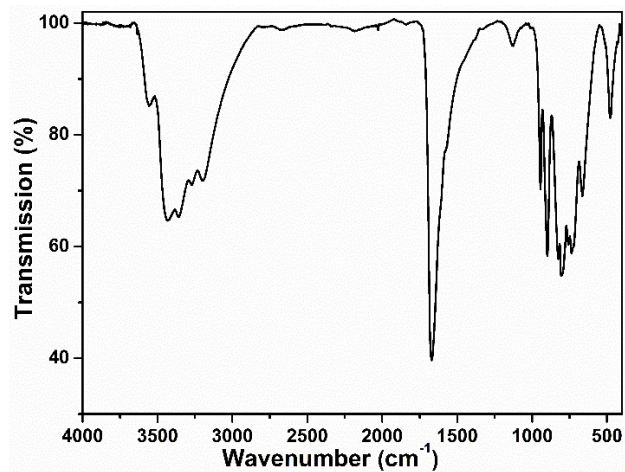


Fig. S5 The IR spectrum of GMIO.

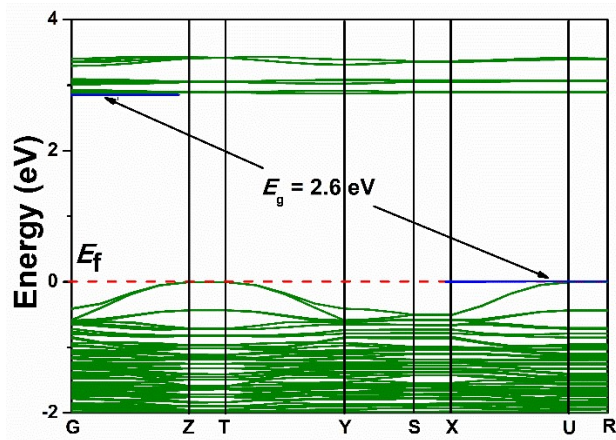


Fig. S6 Calculated band structures for GMIO.

References

1. G. M. Sheldrick, *Acta Crystallogr A*, 2008, **64**, 112-122.
2. G. M. Sheldrick, *University of Göttingen, Germany*, 1997.
3. A. L. Spek, *J. Appl. Cryst.*, 2003, **36**, 7-13.
4. P. Kubelka and F. Z. Munk, *Tech. Phys.*, 1931, **12**, 593-601.
5. J. Tauc, *Mater. Res. Bull.*, 1970, **5**, 721-729.
6. S. K. Kurtz and T. T. Perry, *J. Appl. Phys.*, 1968, **39**, 3798-3813.
7. M. D. Segall, P. J. D. Lindan, M. J. Probert, C. J. Pickard, P. J. Hasnip, S. J. Clark and M. C. Payne, *Journal of Physics: Condensed Matter*, 2002, **14**, 2717-2744.
8. J. P. Perdew, K. Burke and M. Ernzerhof, *Phys. Rev. Lett.*, 1996, **77**, 3865-3868.
9. K. Kobayashi, *Computational Materials Science*, 1999, **14**, 72-76.
10. D. Vanderbilt, *Physical Review B.*, 1990, **41**, 7892-7895.
11. G. Kresse, *VASP*, 5.3.5; <http://cms.mpi.univie.ac.at/vasp/vasp.html>, **2014**.
12. S. N. Rashkeev, W. R. L. Lambrecht and B. Segall, *Phys. Rev. B.*, **1998**, **57**, 3905.
13. B. Champagne and D. M. Bishop, *Adv. Chem. Phys.*, **2003**, **126**, 41-92.
14. A. H. Reshak, S. Auluck and I. V. Kityk, *Phys. Rev. B.*, 2007, **75**, 245120.
15. Y. L. Hu, X. X. Jiang, C. Wu, Z. P. Huang, Z. S. Lin, M. G. Humphrey and C. Zhang, *Chem. Mater.*, 2021, **33**, 5700-5708.
16. Q. M. Huang, C. L. Hu, B. P. Yang, R. L. Tang, J. Chen, Z. Fang, B. X. Li and J. G. Mao, *Chem. Mater.*, 2020, **32**, 6780-6787.
17. T. C. Shehee, R. E. Sykora, M. K. Kang, P. S. Halasyamani and T. E. Albrecht-Schmitt, *Inorg. Chem.*, 2003, **42**, 457-462.
18. X. A. Chen, X. A. Chang, H. G. Zang, Q. Wang and W. Q. Xiao, *J. Alloys Compd.*, 2005, **396**, 255-259.
19. L. Zhang, X. Chen, X. Chang, H. Zang and W. Xiao, *Journal of Synthetic Crystals* 2005, **34**, 812-816.
20. A. H. Reshak and S. Auluck, *J. Alloys Compd.*, 2016, **660**, 32-38.
21. X. A. Chen, L. Zhang, X. N. Chang, H. P. Xue, H. G. Zang, W. Q. Xiao, X. M. Song and H. Yan, *J. Alloys Compd.*, 2007, **428**, 54-58.
22. Y. L. Hu, X. X. Jiang, C. Wu, Z. P. Huang, Z. S. Lin, M. G. Humphrey and C. Zhang, *Chem. Mater.*, 2021, **33**, 5700-5708.
23. R. E. Sykora, K. M. Ok, P. S. Halasyamani and T. E. Albrecht-Schmitt, *J. Am. Chem. Soc.*, 2002, **124**, 1951-1957.